Deep phenotyping of immune cell populations by optimized and standardized flow cytometry analyses

Fabien Pitoiset, Lydie Cassard, Karim El Soufi, Lisa Boselli, Jonathan Grivel, Alexandra Roux, David Klatzmann, Nathalie Chaput, Michelle Rosenzwajg

Deep Phenotyping of Immune Cell Populations by Optimized and Standardized Flow Cytometry Analyses

Fabien Pitoiset,[1,2†] Lydie Cassard,[3†] Karim El Soufi,[1,2] Lisa Boselli,[3] Jonathan Grivel,[3] Alexandra Roux,[1,2] David Klatzmann,[1,2] Nathalie Chaput,[3,4†] Michelle Rosenzwajg[1,2†*]

[1]Sorbonne Universités, UPMC Univ Paris 06, INSERM, UMR S 959, Immunology-Immunopathology- Immunotherapy (I3), F-75005, Paris, France

[2]Biotherapy (CIC-BTi) and Inflammation-Immunopathology-Biotherapy Department (DHU i2B), Hôpital Pitié-Salpêtrière, AP-HP, F-75651, Paris, France

[3]Laboratory of Immunomonitoring in Oncology, Gustave Roussy Cancer Campus, CNRS-UMS 3655 and INSERM-US23, Villejuif, F-94805, France

[4]Faculty of Pharmacy, University Paris-Sud, Chatenay-Malabry, F-92296, France

Received 11 December 2017; Revised 28 June 2018; Accepted 2 July 2018

Grant sponsor: ANR (French Government Investissement d'Avenir programme [Labex Transimmunom]), Grant number: ANR-11-IDEX-0004-02; Grant sponsor: Gustave Roussy Cancer Campus; Grant sponsor: Fondation Gustave Roussy; Grant sponsor: SIRIC SOCRATE, Grant number: INCa DGOS INSERM 6043; Grant sponsor: MMO program, Grant number: ANR-10IBHU-0001; Grant sponsor: European Research Council Advanced Grant [TRiPoD], Grant number: FP7-IDEAS-ERC-322856; Grant sponsor: ANR (Recherche Hospitalo-Universitaire en santè [RHU Imap - towards low-dose iL-2 Market APproval for autoimmune diseases]), Grant number: ANR-16-RHUS-0001

Additional Supporting Information may be found in the online version of this article.

[†]These authors contributed equally to this work.

[*]Correspondence to: Dr. Michelle Rosenzwajg, Pierre & Marie Curie University and Medical school, Service de Biothérapies, UMRS 959 UPMC/INSERM, Hôpital de la Pitié Salpétrière, CERVI 2é, 83 bd de l'Hôpital 75651, Paris Cedex 13, France
Email : michelle.rosenzwajg@upmc.fr#

Abstract

Multicolor flow cytometry is a technology of choice for phenotyping of immune cells, and it can be used routinely for the follow up of patients in clinical trials. But it is challenging to define combinations of conjugated antibodies that efficiently allow the detailed analysis of major immune cell subsets and the identification of rare cell populations. In a collaborative work among the Immunology, Immunopathology, Immunotherapy (I^3) laboratory, and the laboratory of immunomonitoring in oncology (L.I.O), we developed and validated 12 different 10-color flow cytometry panels that allow the deep immunophenotyping of cells from whole blood for the follow up of autoimmune and cancer patients. Here, we describe these optimized flow cytometry panels, showing that they provide the advanced analysis of T cells (including regulatory T cells), B cells, NK cells, MAIT cells, myeloid cells, monocytes, and dendritic cells. Most of the panels have been dried to improve standardization of the labeling and the entire procedure can be performed on less than 2 ml of whole blood. These deep immunophenotyping flow cytometry panels constitute a powerful tool for the monitoring of immune blood cells and will hopefully lead to the discovery of new biomarkers and potential therapeutic targets in autoimmune and cancer clinical trials.

Key terms

human immunology; flow cytometry; immunomonitoring; immunophenotyping; deep phenotyping; clinical studies

In clinical trials, analysis of immune cell populations is becoming more and more prevalent, especially in studies focusing on pathologies related to immune disorders, either exacerbated immune system activation leading to autoimmunity (1), or in contrast insufficient or inadequate immune responses allowing the growth of tumors (2); but also in cohorts of patients treated with immunotherapies such as in oncology (3). Despite the success of immunotherapy in autoimmune diseases or cancer, clinically actionable biomarkers to aid patient and regimen selection are lacking and well-validated biomarkers that can be effectively implemented in the clinic are required (4).

Flow cytometry has become the technology of choice for the monitoring of immune cells as it provides the possibility to analyze a large number of parameters simultaneously, in a short time and for a reasonable cost rendering flow cytometry feasible for a routine clinical use. Therefore, many cell subsets can be identified, but it requires establishing complex combinations of conjugated antibodies to optimally distinguish populations of interest (5). With the increasing number of available antibodies and the new generation of cytometers, the frequent description of new subpopulations, and new discoveries about the role of different cell subsets or molecules in pathologies, it is a time-consuming and challenging process to define relevant and optimized panels of flow cytometry for clinical trials and translational research (5).

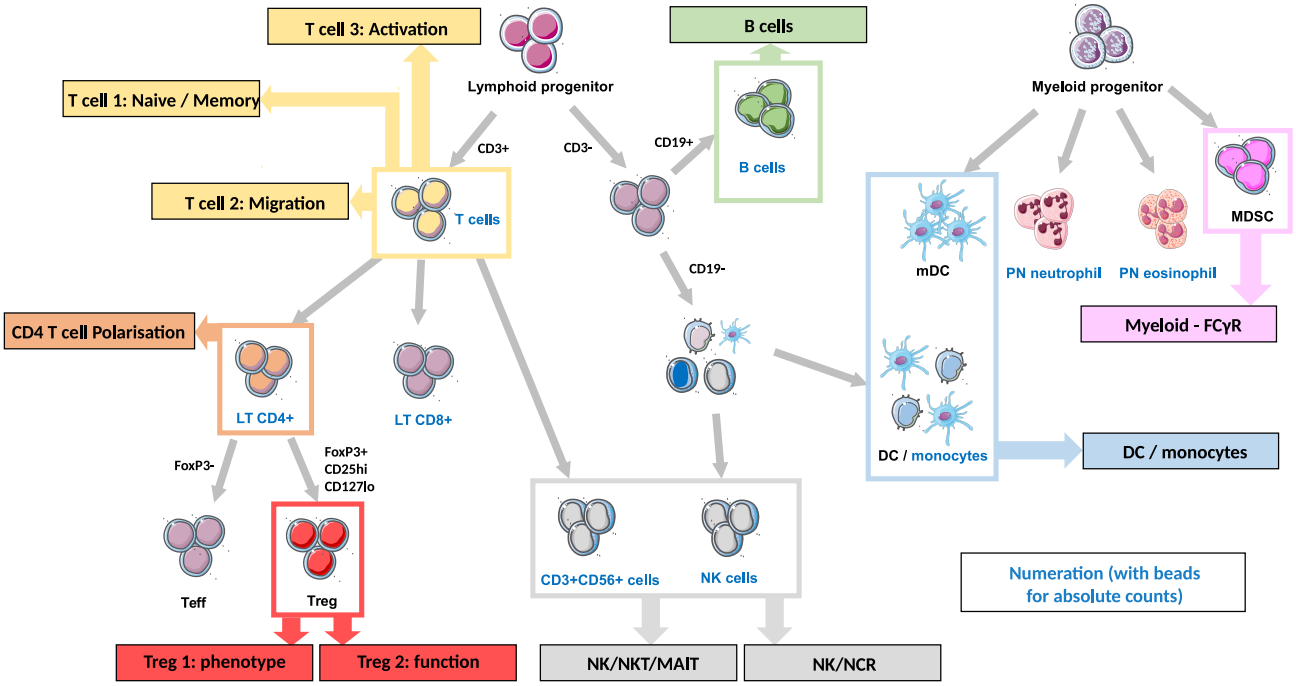

Figure 1. Schematic representation of the populations targeted by the flow cytometry deep immunophenotyping. Each colored and framed population name is studied by a specific panel. The Numeration panel, represented in the white frame, contains counting beads and allows the identification and quantification of all populations annotated in blue. [Color figure can be viewed at wileyonlinelibrary.com]

The Transimmunom initiative is a large observational study conducted in the I^3 laboratory in La Pitié-Salpêtrière hospital aiming at deciphering the autoimmune and inflammatory diseases. Nosography of these pathologies is still based today, nearly exclusively on clinical symptoms (6). Our objective is to identify immunological characteristics that would allow to cut across diagnostic groups and reconsider current disease classification schemes. In that goal, we aim to include a 1,000 patients distributed into groups of 100 depending on the selected pathology plus 100 healthy donors. For each donor/patient, a large number of omics will be performed, such as transcriptomics, proteomics, genomics, microbiota, TCR repertoire, and deep immunophenotyping. This cross-phenotyping will allow us to discover and validate biomarkers and novel therapeutic targets, which in turn will benefit diagnosis and treatment. We hope the knowledge that will stem out of this endeavor will give rise to the development of new biotherapies (7).

The primary goal of L.I.O at Gustave Roussy Institute is to better characterize the immune status of cancer patients longitudinally before and after introduction of immune checkpoints blockers (ICB). One of our objectives is to identify immunological characteristics before and after introduction of ICB that would predict clinical responses and/or ICB-induced immune-related adverse events (IrAE) in cancer patients (8). As in the Transimmunom consortium, a large number of omics will be performed in cancer patients in a longitudinal way (9). Finally, we predict that comparison of cancer patients developing IrAE during ICB treatment and patients from the Transimmunom consortium could help to better understand the onset of autoimmunity and/or inflammatory diseases.

For each of the panels described thereafter, 10 markers were selected in accordance with experts' opinion and literature, in particular Optimized Multicolor Immunofluorescence Panels (10) and Human Immunology Project Consortium (11) recommendations, to efficiently be able to gate on populations of interest and to have the most informative markers being analyzed on all cell subsets. Here, we describe this large set of optimized and standardized 10-color flow cytometry panels of conjugated antibodies in ready-to-use tubes, developed in collaboration between I^3 laboratory and L.I.O. These immunophenotyping procedures allow a deep phenotyping of most of the known immune cell populations in whole blood, therefore, representing a powerful tool for immunological investigations in clinical trials.

Results

Design of the Panels

The first step of the panels design consisted in the identification of cell populations or functions of cells of interest, which led to a choice of 12 different panels (Fig. 1). Six panels were designed for the study of T cells, as they represent key populations in immune-related pathologies. More precisely, we allocated three panels to study activation, migration, and memory phenotype of T cells, one panel was dedicated to the analyze of $CD4^+$ T-cells polarization, while two panels

focused on the phenotype of regulatory T cells, one of which comprising an intracellular staining for the FoxP3 marker that is essential to optimally discriminate regulatory T cells. In the second Treg panel, regulatory T cells were gated as $CD4^+CD127^{lo/-}CD25^+$ without the FoxP3 to allow the evaluation of a maximum of functional markers. Other panels aimed at investigating B cells, NK cells, monocytes and dendritic cells, MAIT cells, and myeloid-derived suppressor cells. Importantly, we also designed an additional panel allowing the identification of principal immune cell populations and including numeration beads, which made it possible to measure the absolute counts of all populations, while serving as a reference tube that allows the calculations of absolute counts in all other panels by extrapolation from shared populations.

After selection of 10 target markers for each of these panels in accordance with literature, next step consisted in selecting fluorochrome combinations, to maximize the quality of staining. To achieve that, numerous combinations of antibody-fluorochromes were tested in collaboration with Beckman Coulter, Inc. in accordance with flow cytometry panel design rules(12) to optimize the separation of positive populations for each marker, while keeping compensations to reasonable levels. Each antibody was titrated based on achieving the highest signal (mean fluorescence intensity) for the positive population and the lowest signal for the negative population representing the optimal signal to noise ratio. As a result, we selected 97 conjugated antibodies composing 12 different panels in liquid formulation. The resulting panels of antibody-fluorochrome combinations are presented in Table 1.

In this study, whole blood staining was preferred to peripheral blood mononuclear cells (PBMC) to reduce technical manipulations and the blood sampling needed to perform the tests. This allows the entire procedure with the 12 panels to be performed on less than 2 ml of blood. Moreover, working on whole blood avoids the loss or reduction or phenotype modifications of some cell subsets (granulocytes (13,14), dendritic cells (14), monocytes (14), lymphocytes (15–17)) that happen during PBMC isolation or freezing. These cells can be of major importance and ultimately poorly studied because of their short lifespan after blood sampling (granulocytes) or their absence or very low proportion in PBMCs (granulocytes and dendritic cells, respectively).

Furthermore, to standardize the staining procedures, we decided to use the Duraclone® technology, which provides the possibility to produce custom designed panels of antibodies that are dried and pre-coated in individual tubes for direct labeling of blood (18–20). This technology was used to reduce the number of technical steps and avoid a maximum of biases, as it ensures the exact same quantity of antibodies from the same batch and it is very stable overtime (one and a half year certified by the manufacturer). Notably, not all antibodies could be dried, for intellectual property reasons or impossibility to dry some fluorochromes such as Brilliant Violet and Ultraviolet. As a result, majority of clones from Beckman Coulter and Biolegend catalogs were dried and included in the Duraclone tubes, but clones from Becton Dickinson, R&D System and eBioscience were excluded from

Table 1. Composition of the 12 panels

	FITC	PE	ECD	PE-Cy5.5	PC7	APC	AA700	AA750	PB	KRO
Numeration	CD 16	CD56	CD19	CD244	CD 14	CD8	CD4	CD3	CD15	CD45
T cell 1	CD95	CCR7	HLA-DR	CD25	CD45RA	ICOS	CD3	CD127	CD4	CD8
T cell 2	CLA	CD49a	CCR7	β7 integrin	CD45RA	CD103	CD3	CD49d	CD4	CD8
T cell 3	CD57	CD160	CD69	PD-1	CD 137	OX40	CD3	CDS	CD4	CD8
CD4 T-cell polarization	CXCR3	CCR10	CCR7	CCR6	CCR4	CXCR5	CD3	CD45RA	CD4	CD 161 or PD-1
Treg 1 (liquid)	Helios	CD25	iCXCRS	Ki67	CTLA-4	Foxp3	CD8	CD127	CD4	CD3
Treg 2 (liquid)	LAP	GITR	CD25	CD39	CD45RA	LAG-3	CD3	CD 127	CD4	CD8
B cells	IgD	CD10	CD5	CD27	CD38	IgM	CD19	CD24	CD21	CD32
MAIT cells/NKT	TCR Va 7.2	CD 54	HLA-DR	CD56	TCR-Va2.4	TCR-Vβll	CD3	CD 161	CD4	CD8
NK/NCRs	TCRγδ	NKp44	HLA-DR	NKp30	NKp46	NKG2D	CD3	CD 16	CD56	CD8
DC/monocytes	CD 16	CCR5	CD14	BDCA-3	CD1c	CD123	LIN CD3-CD19-CD56	CD11c	HLA-DR	CD45
Myeloid/FcγRs	CD16	-	HLA-DR	CD244	CD64	CD33	CD14	CD11b	CD15	CD32

Fluorochromes indicated in the column title are classical fluorochromes from Beckman Coulter. See Supporting Information Table S1 for details (antibody clones, manufacturers, and volumes).

FITC, fluorescein isothiocyanate; PE, phycoerythrin; ECD, PE-Texas-Red; PE-Cy5.5, PE-Cyanin 5.5; PC7, PE-Cyanin 7; APC, Allophycocyanin; AA700, APC-Alexa Fluor 700; AA750, APC- Alexa Fluor 750; PB, Pacific Blue; KRO, Krome Orange.

the dried formulation and are added as dropped antibodies (see Supporting Information Table S1 for details). For each of the antibody panels, a pre-lot of Duraclone tubes was produced and their reproducibility (percentages of population of interest and fluorescence intensities) with the liquid staining was validated, before the production of Duraclone tubes. No significant differences could be noted between dry and liquid formulation for most subsets and proportion of main immune subsets remained highly correlated (Supporting Information Fig. S1A–C and not shown). However, dry formulation led in some case to higher fluorescence intensity in comparison with the liquid cocktail allowing a better discrimination of some subpopulations such as $CCR7^+$ central and effector memory T cells; yet this populations remained highly correlated (see Supporting Information Fig. S1D–F). For unknown reasons, the two panels focused on Tregs as well as PerCPCy5.5-conjugated anti-CCR6 ab from Biolegend did not pass this validation process, because Duraclone pre-lots failed to reproduce the labeling obtained with their liquid counterparts. Thus, Treg panels have been conserved in liquid format and PC5.5-coupled anti-CCR6 ab was dropped in "T cell polarization" panel for the study.

For standardization of the cytometer parameters, in addition to the flow set pro and flow check beads that are used daily as quality control, 8-peaks fluorescent beads were used before each acquisition. For each acquisition channel, target values for a specific peak were determined, and amplifications were modified to keep signals stable over time. Compensations were performed with VersaComp Ab capture beads and Duraclone single staining tubes for each dried antibody, or liquid single staining for others. This was performed once at the beginning of the study, and then again when modifications were brought to the cytometer (e.g., in the case of maintenance). Importantly, all along the Transimmunom trial or for patients with cancer at Gustave Roussy Cancer Campus, the same cytometer, a Gallios (Beckman Coulter) dedicated to the study, was used. Altogether these features ensure consistency in the assays and guarantee the possibility of comparing samples acquired longitudinally.

For all panels, doublet cells, dead cells, and debris are removed from the analysis using the forward and side scatters areas, widths, and heights, as shown in Supporting Information Figure S2.

Description of Panels

In the "numeration" panel, we chose to include anti-CD45 to isolate all leucocytes, anti-CD19 and anti-CD3 to discriminate B and T cells, respectively, anti-CD4 and anti-CD8 to discriminate $CD4^+$ and $CD8^+$ T cells among $CD3^+$ T cells, anti-CD56 to study NK and NKT cells, anti-CD14 for monocytes, anti-CD15 for neutrophils and eosinophils, and anti-CD16 and anti-CD244 to differentiate eosinophils from neutrophils among the $CD15^+$ population. Anti-CD16 is also used to discriminate subsets of monocytes and NK cells. The gating strategy for this tube is presented in Figure 2. In this panel, no wash is performed after the staining, thus avoiding the eventual modification of any cell population in the wash process, and count beads are added prior to acquisition, raising absolute counts in addition to percentages. These counts were compared with results obtained from a clinical kit (TetraCXP System from Beckman Coulter, Inc.). Correlation between the two techniques is very high (Supporting Information Fig. S3), thus validating the reliability of absolute counts obtained with the Numeration panel. These absolute counts are used to extrapolate absolute numbers in every other panel by using markers shared with this panel.

In each of the six panels dedicated to analysis of T cells and described hereafter, anti-CD3 antibody is present to gate on T cells, and anti-CD4 and anti-CD8 allow the discrimination of $CD4^+$ and $CD8^+$ T cells. Hence only the seven other antibodies are described for these six panels.

The "T cell 1" panel contains anti-CD45RA and anti-CCR7 antibodies, allowing the identification of naïve/Stem Memory T cells ($CD45RA^+CCR7^+$), central memory (CM, $CD45RA^-CCR7^+$), effector memory (EM, $CD45RA^-CCR7^-$), and effector memory RA (TEMRA, $CD45RA^+CCR7^-$) populations. Anti-CD95 is used to discriminate naïve cells among naïve $CD45RA^{high}CCR7^{high}$ cells from memory stem T cells that are long-lived lymphocytes able to persist in the host in the absence of antigen and were shown to provide a potential reservoir for T-cell memory throughout life (21). Anti-ICOS and anti-HLA-DR has been added to this panel for the evaluation of the activation status of each subset of T cells. Importantly, we also included anti-CD25 and anti-CD127 antibodies to evaluate the differentiation and activation status of regulatory T cells ($CD4^+CD25^+CD127^{lo/-}$). The gating strategy is represented in Supporting Information Figure S4.

The "T cell 2" panel contains five antibodies directed against molecules known to favor the migration of T cells and to address them to specific tissues: CLA (cutaneous leucocyte-associated antigen for skin homing), CD103 and β7-integrin or $\alpha E^+\beta7^+$ (mucosal tissues and mucosal tumors), CD49d and β7-integrin or $\alpha4^+\beta7^+$ (gut homing) and CD49a or α1 mucosal integrin. CD45RA and CCR7 are also present to allow analyses of the expression of migration molecules separately on different naïve/memory subsets of $CD4^+$ and $CD8^+$ T cells. Supporting Information Figure S5 shows an example of the staining and gating strategy.

The "T cell 3" panel contains seven different antibodies directed against activation (CD69, CD137/4-1BB, and CD134/OX40), negative modulator of the TCR (CD5) (22), exhaustion such as immune checkpoints (PD-1, CD160) (23) or senescence (CD57) (24) molecules. Expression of these molecules is analyzed separately on $CD4^+$ and $CD8^+$ T cells. An example of gating strategy is represented in Supporting Information Figure S6.

In the "T cell polarization" panel (Fig. 3), antibodies directed against chemokines receptors (CCR6, CCR10, CXCR4, and CXCR3) are then used to discriminate Th1, Th2, Th17, and Th22 subsets (25), among TfH (defined as $CXCR5^+$) (Fig. 3A) and memory helper T cells ($CD45RA^{lo/-}$; Fig. 3B) populations, anti-CCR7 being added to study the CM and EM phenotype in each Th subset (Fig. 3C). Notably, in this panel, either CD161 (to discriminate Th9 from Th17.1 cells, as shown in Fig. 3) or PD-1 (to better discriminate Tfh

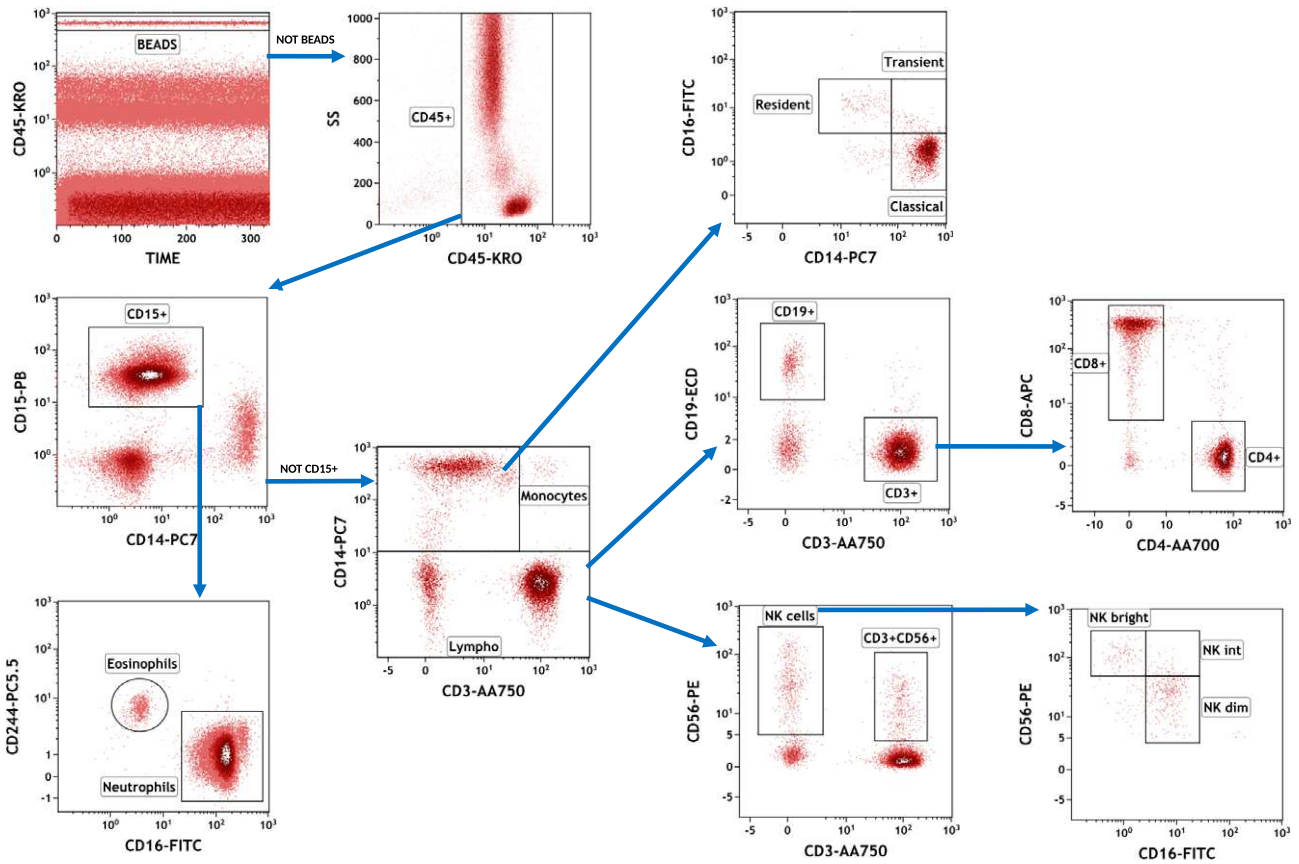

Figure 2. Gating strategy for the "Numeration" panel. Beads are excluded on a TIME/CD45 dot plot. Leukocytes ($CD45^+$ cells) are then gated on a CD45/SS dot plot. Granulocytes ($CD15^+$) cells are gated on a CD14/CD15 dot plot and eosinophils ($CD16^-CD244^+$) and neutrophils ($CD16^+CD244^-$) are discriminated using CD16 and CD244 expression levels. Lymphocytes ($CD14^-$) and monocytes ($CD14^+CD3^-$) are separated on a CD3/CD14 dot plot gated on $CD15^+$ cells. Different subsets of monocytes are identified on a CD14/CD16 dot plot. Gated on the lymphocyte population, T cells ($CD3^+CD19^-$) and B cells ($CD3^-CD19^+$) are gated on a CD3/CD19 dot plot, and NK cells ($CD3^-CD56^+$) and $CD3^+CD56^+$ are gated on a CD3/CD56 dot plot. $CD4^+$ T cells and $CD8^+$ T cells are separated from the T-cell population, and different subsets of NK cells are distinguished using CD16 and CD56 expression levels. [Color figure can be viewed at wileyonlinelibrary.com]

cells) can be dropped (not shown). The memory phenotype can then be assessed on the basis of the CD45RA and CCR7 expressions (Fig. 3D).

The "Treg 1" panel (Supporting Information Fig. S7) aims to characterize the regulatory T cell population (Treg). Anti-FoxP3, anti-CD25, and anti-CD127 are used to gate on Tregs (defined as $CD4^+FoxP3^+CD25^+CD127^{lo/-}$ cells). Other phenotypic markers (Helios, CXCR5, and CTLA-4) complete this panel to define more precisely subsets of Tregs. Ki67 is used to evaluate the presence of cycling Tregs. Notably, $CD8^+$ Tregs, which can express CTLA-4 and Ki67 (26), can also be evaluated for their expression of these phenotypic markers with this panel (not shown).

The "Treg 2" panel (Supporting Information Fig. S8) was designed to go further into the functionality and activation of regulatory T cells. Anti-CD25 and anti-CD127 are used to gate on Tregs (defined here as $CD4^+CD25^+CD127^{lo/-}$). Although it is not optimal for identification of Tregs to use only CD25 and CD127, we previously showed that percentages of $FoxP3^+$/$CD25^+/CD127^-$ and $CD25^+/CD127^-$ are highly correlated (27). And avoiding to add FoxP3 in some panels in which we focus on Tregs (1) grants us the possibility to add an additional phenotypical marker in each panel, and (2) avoids the necessity to perform an intracellular staining, thus accelerating and simplifying the procedure. Functional/activation markers chosen in this panel were LAP, GITR, CD39, CD45RA, and LAG-3. Anti-CD45RA is also used to analyze the expression of the other markers separately on naïve and activated Tregs.

The "B cells" panel (Fig. 4) allows evaluation of the differentiation status and phenotypic characterization of B cells. In that purpose, anti-CD19 is used to gate on B cells, and anti-IgD, anti-IgM and anti-CD27 let us discriminate naïve mature B cells ($IgD^+IgM^+CD27^-$) from unswitched ($IgD^+IgM^+CD27^{+)}$ and switched ($IgD^-IgM^-CD27^+$) memory B cells. Anti-CD24 and anti-CD38 antibodies are used to identify transitional B cells ($CD24^{hi}CD38^{hi}$) and plasmablasts ($CD24^-CD38^{high}$). Other markers that have been selected to define with more precision subsets of B cells (28) are CD21 (for $CD21^-$ B cells), CD5, CD10 (for pre- and pro-B cells), and CD32 (FcγRII) for regulation of B cell functions.

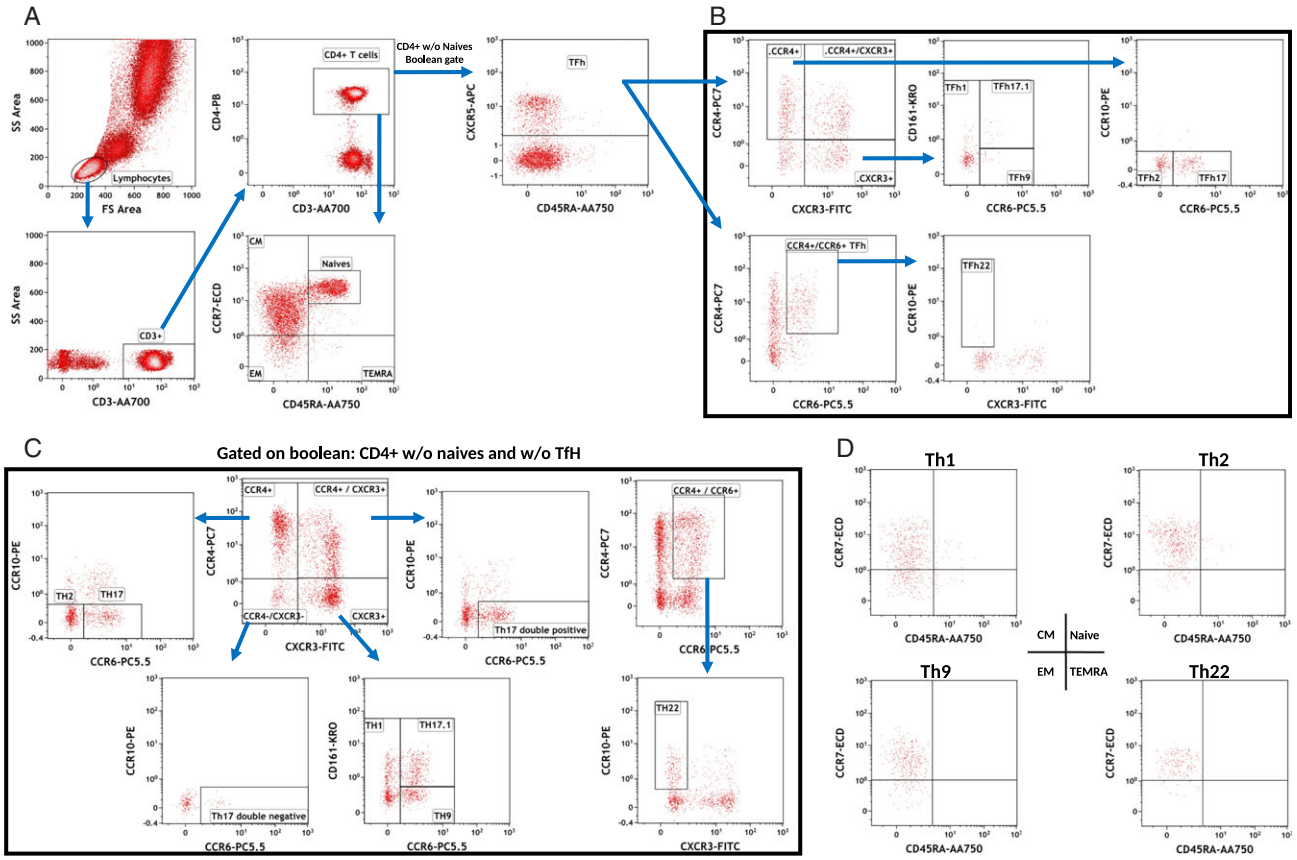

Figure 3. Gating strategy for the "CD4 T cell polarization panel." (**A**) Lymphocytes are gated on a FS/SS dot plot, $CD4^+$ T cells ($CD3^+CD4^+$) are gated on a CD3/CD4 dot plot and naive $CD4^+$ T cells ($CD45RA^+CCR7^+$) are identified on a CD45RA/CCR7 dot plot. Gated on $CD4^+$ and not naive (boolean gate) cells, TfH cells are identified on a CXCR5/CD45RA dot plot. (**B**) Identification of the TfH subsets. Gated on TfH cells, $CXCR3^+$ and $CCR4^+$ cells are gated on a CXCR3/CCR4 dot plot. TfH1 and TfH9 and TfH17.1 (among $CXCR3^+$ cells) and TfH2 and TfH17 (among $CCR4^+$ cells) subsets are then discriminated on CCR6/CD161 and CCR6/CCR10 dot plots, respectively. (**C**) Identification of the TH subsets. Gated on $CD4^+$ and not naives and not TfH cells (boolean gate), TH1 ($CXCR3^+CCR4^-CCR6^-CCR10^-$), TH9 ($CXCR3^+CCR4^-CCR6^+CCR10^-CD161^-$), TH17.1 ($CXCR3^+CCR4^-CCR6^+CCR10^-CD161^+$), TH2 ($CXCR3^-CCR4^+CCR6^-CCR10^-$), TH17 ($CXCR3^-CCR4^+CCR6^+CCR10^-$), TH17 double positive ($CXCR3^+CCR4^+CCR6^+CCR10^-$), TH17 double negative ($CXCR3^-CCR4^-CCR6^+CCR10^-$), and TH22 ($CCR4^+CCR6^+CXCR3^-CCR10^+$) subsets are identified as indicated. (**D**) Naive memory subsets of TH cells. Gated on major TH subsets, the naive/memory phenotype ($CD45RA^+CCR7^+$ naive cells, $CD45RA^-CCR7^+$ CM cells, $CD45RA^-CCR7^-$ EM cells, $CD45RA^+CCR7^-$ effector memory RA [TEMRA] cells) is analyzed based on the expression of CD45RA and CCR7. [Color figure can be viewed at wileyonlinelibrary.com]

The "MAIT cells/NKT" panel (Supporting Information Fig. S9) contains anti-HLA-DR to exclude from analysis B cells and potential contaminating antigen presenting cells, and anti-CD4 to exclude monocytes. Anti-CD3 and anti-CD56 are used to gate on NKT cells ($CD3^+CD56^+$), among which we can identify type 1 NKT expressing TCR-Vα2.4 and TCR-Vβ11. Anti-TCR-Vα7.2 and anti-CD161 allow the identification of MAIT cells (TCR-$V\alpha7.2^+CD161^+$), and anti-CD8 is used to discriminate "true" MAIT cells that express CD8. In this panel, expression of CD54 (ICAM-1) on NK cells is also evaluated to determine CD16-engagement in patients treated with therapeutic monoclonal antibodies engineered to enhance antibody-dependent cell cytotoxicity (29).

The "NK/NCR" (Supporting Information Fig. S10) has been designed mainly to focus on NK cell subsets and evaluate their phenotype and activation status. Anti-CD56 antibody is used to discriminate NK and NK bright cells. Expressions of NK cell receptors (NKG2D, NKp30, NKp44, and NKp46), CD16, CD8, and HLA-DR are then evaluated on NK cells (Supporting Information Fig. S10A). Expression of some of these molecules is also evaluated on $CD3^+CD56^+$ cells (Supporting Information Fig. S10B), $CD8^+$ T cells (Supporting Information Fig. S10C), and TCRγδ T cells (Supporting Information Fig. S10D).

The "DC/monocytes" (Supporting Information Fig. S11 panel contains anti-CD45 to isolate mononuclear cells for analysis. Then with anti-CD3/CD19/CD56 lineage and anti-HLA-DR, we isolate the dendritic cell and monocyte populations ($CD3^-CD19^-CD56^-$HLA-DR^+), and $CD3^-CD19^-CD56^-$HLA-DR^-. Among Lin^-HLA-DR^+ cells, anti-CD123, and anti-CD11c allows the discrimination of plasmacytoïd dendritic cells ($CD11c^-CD123^+$), and of the myeloid compartment ($CD11^+CD123^-$ cells). In this compartment, the myeloid dendritic cells ($CD14^-CD16^-$) can be discriminated

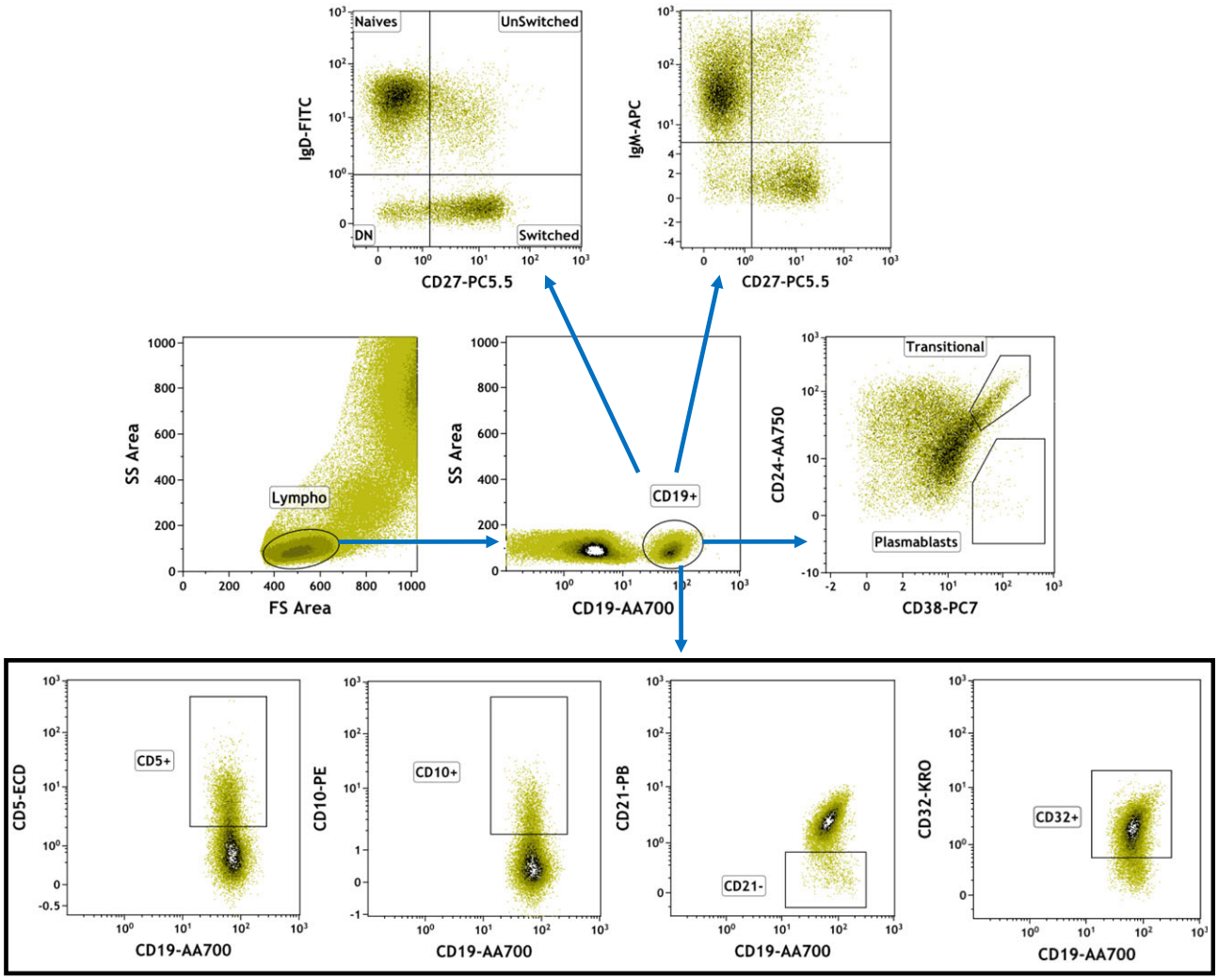

Figure 4. Gating strategy for the "B cells" panel. The lymphocyte population is gated on a FS/SS dot plot, and B cells ($CD19^+$) are identified on a CD19/SS dot plot. The differentiation status (naive ($CD27^-IgD^+IgM^+$), unswitched ($CD27^+IgD^+IgM^+$) or switched [$CD27^+IgD^-IgM^-$]) of B cells is evaluated either on a CD27/IgD or a CD27/IgM dot plot. Transitional B cells and plasmablasts are discriminated on a CD38/CD24 dot plot, and $CD5^+$, $CD10^+$, $CD21^-$, and $CD32^+$ B cells are gated on a CD19/CD5, a CD19/CD10, a CD19/CD21, and a CD19/CD32 dot plot, respectively. [Color figure can be viewed at wileyonlinelibrary.com]

from the different monocyte populations on a CD14/CD16 plot. Among mDCs, anti-CD141, and anti-CD1c are used to separate mDC1 ($CD1c^+CD141^-$) and mDC2 ($CD1c^-CD141^+$). Anti-CCR5 is used to study the expression of CCR5 on mDCs. It is also possible in this panel to evaluate basophils ($Lin^-HLA\text{-}DR^-CD123^+CD45^{dim}$) among the $Lin^-HLA\text{-}DR^-$ population based on the expression of CD123 and a dim expression of CD45 (30).

The "Myeloid - FcγR" panel (Supporting Information Fig. S12) is composed of an anti-HLA-DR used as exclusion markers, anti-CD11b, anti-CD33, anti-CD14, and anti-CD15 are used to identify monocytic myeloid-derived suppressor cells ($CD11b^+CD33^+CD14^+CD15^-$, Supporting Information Fig. S12A). This panel is also used to evaluate the expression of HLA-DR and Fcγ receptors (CD16, CD32, and CD64) at the surface of different subsets of monocytes ($CD14^+CD16^-$, $CD14^+CD16^+$ or $CD14^{lo/-}CD16^+$, Supporting Information Fig. S12B), neutrophils ($CD15^+$ $CD244^-$, Supporting Information Fig. S12C), and eosinophils ($CD15^+$ $CD244^+$, Supporting Information Fig. S12D).

As an interpanel validation, we evaluated the coefficient of variability (CV) of measurements of populations that are shared by different panels (Supporting Information Fig. S13A). For all populations, the mean of the CVs was low (all below 15% except for one), thus highlighting the consistency of results obtained from the different panels. The only exception was the eosinophil population that yielded slightly higher CVs, due to the fact that little variations in measurements can dramatically increase the CV in less represented population. For interpanel validation of the regulatory T cells measurement, we evaluated the correlation between the values obtained with or without the FoxP3 marker (Supporting Information Fig. S13B). As already shown, a strong correlation was observed between

FoxP3$^+$CD25$^+$CD127$^-$ and CD25$^+$CD127$^{lo/-}$ cells among CD4$^+$ cells (27).

The 12 flow cytometry panels have already been implemented in our labs, as more than 150 patients and donors have already been recruited in the Transimmunom project, and preliminary analyses have already yielded interesting results, confirming the interest of our approach. All the panels described in this article allow the generation of more than 700 data per patient, including percentages of parent population, absolute count of cells, and mean fluorescence intensities.

Discussion

We designed a set of 12 10-color flow cytometry panels that provides a detailed description of immune cells in the blood of patients. In comparison with other reference studies such as the ONE study (31) or the Milieu Intérieur consortium (32), we made the choice to design more exhaustive panels and are capable to define a deeper phenotyping of various cell subsets. The main reason for this is the number of panels and the number of colors used within the panels (12 10-color panels in our study versus six panels with 7–9-colors for the ONE study and four panels with 7–10 colors for the Milieu Intérieur). In particular the six panels dedicated to T cells provide a very advanced phenotype of T cell subsets which play a key role in autoimmune diseases, and to our knowledge, we are the only group studying NK cells in details, MAIT cells, non-conventional T cells or myeloid cells in a general immunophenotyping approach like this one. Moreover, we are currently developing an additional panel aiming at identifying the different subsets innate lymphoid cells, which are thought to be involved in multiple autoimmune diseases (33).

Dried reagents have already proven to yield high reproducibility and efficient standardization in large-scale projects such as the ONE study (31) and the PreciseADS study (20). Similarly, the use of such dried reagents in this fine immunophenotyping represents an advantage for reliability of data, but also to speed up and simplify the labeling technique. The use of counting beads providing reliable absolute counts of cell populations is another valuable advantage in patients follow up.

Mass cytometry or CyTOF, arose in the last years and could have represented an alternative solution to perform the deep immunophenotyping in our studies. But multiple reasons led us to choose flow cytometry including: (1) the time acquisition with CyTOF that is much slower (a maximum of around 1,000 events per second) that would not be suitable for routine use or for a trial like Transimmmunom or clinical trials including patients treated with ICB as at Gustave Roussy for cancer patients in which up to eight fresh whole blood samples from patients can be analyzed rapidly the same day; (2) the limited catalog (albeit growing) of commercial antibodies; (3) the absence of FSC/SSC equivalents in mass cytometry, as cells are vaporized; (4) the limitation for the number of antibodies that can be used on the same population: for example our deep immunophenotyping includes 32 different targets for T cells only, which is too much for mass cytometry, because of the steric hindrance; (5) the cost of mass cytometry, which remains today significantly higher than that of flow cytometry; (6) environmental issues (because of elimination of heavy metal elements).

This optimized deep immunophenotyping has already been performed on more than 150 patients/donors in Transimmunom project in the I^3 laboratory and in cancer patients across several clinical trials at L.I.O at Gustave Roussy Institute. It provides a huge amount of data and gives the opportunity to identify cell subsets that are altered in the studied pathologies, and to define some flow cytometry signatures specific for a pathology; a subgroup of patients and/or a response to treatment. Given the quantity of generated data, it is also possible to consider flow cytometry data as omics, and to use big data tools, such as dimension reduction algorithms, to facilitate the analysis. We are currently working on this kind of approach which might lead to the discovery of new cell subsets (e.g., with unexpected combination of marker expressions), therefore representing a powerful tool for immunological investigations in clinical trials. Flow cytometry data can also be integrated in multiscale analyzes with other omics that is, transcriptomic, microbiome, proteomic, and so on, allowing to look for potential signatures composed of data originating from different techniques performed in a trial. This could give the opportunity to revisit the classification of diseases, identify potential therapeutic targets, and develop new biotherapies in autoimmunity as well as in cancers.

These flow cytometry panels can be implemented in other clinical trials, and thanks to the robustness and the efficient standardization of the staining, different studies could be compared in cross-analyses. Moreover, we are currently working on the validation of these panels on fresh or frozen peripheral mononuclear cells, so we can overcome the unavailability of fresh blood in some studies. In the near future, we also plan to transpose these protocols to tissue-derived cells, to be able to compare immunomics from different tissues, or to perform deep immunophenotyping on cells deriving from relevant tissues in the context of specific pathologies. Notably, the deep immunophenotyping in tissues could be of great interest in cancer-related studies wherein a thorough study of T-, B-, NK, and myeloid cells in tumor or affected tissues could yield valuable results.

Material and Methods

Blood Samples

Blood samples from healthy donors were obtained from the French blood bank (Etablissement Français du Sang; agreement No 12/EFS/079) according to ethical guidelines and were collected in Heparin, or from healthy donors participating to the Transimmunom trial (ANR-11-IDEX-0004-02, approved by local ethic committee). Informed consent was obtained from each volunteer.

Antibody Staining

For the "Treg 1" panel CD25-PE, CTLA-4-PECy7, FoxP3-APC, CD8-AA700, CD127-AA750, CD4-Pacific Blue, and CD8-Krome Orange conjugated antibodies are from Beckman Coulter. Helios-FITC was from eBioscience, CXCR5-PE-Dazzle 594 from Biolegend and KI67-PerCPCy5.5 from Becton Dickinson. PerfixNC kit was purchased from Beckman Coulter. Whole blood (100 µl) sampled with anticoagulant was mixed with 10 µl of Perfix-NC R1 buffer, vortexed immediately for 2–3 s and incubated for 15 min at room temperature in the dark. About 600 µl of Perfix-NC R2 buffer were added, 355 µl were transferred in the Duraclone tube and liquid antibodies were added. After vortexing, tubes were incubated for 60 min at room temperature in the dark. PBS 1× (3 ml) was added to the tubes, incubated for 5 min at room temperature in the dark before centrifugation for 6 min at 250*g*. The supernatant was removed to leave the pellet dried and the cells were resuspended in 3 ml of 1× Perfix-NC R3 buffer prior to another 6-min centrifugation at 250*g*. The pellet was dried and resuspended in 300 µl of 1× R3 buffer. Tubes were protected from light and stored at 4°C until the acquisition on a cytometer within the next 24 h.

For all other panels, all conjugated antibodies were dried in Duraclone tubes except for the "Treg 2 panel" and dropped antibodies (see Supporting Information Table S1). Versalyse was purchased from Beckman coulter. For each panel except for "B cells" panel, 100 µl of whole blood were added in the corresponding Duraclone and the liquid antibodies were added when necessary. Notably, for the "B cells" panel, 300 µl of blood were washed twice in PBS 1× prior to staining to remove soluble IgM. After vortex, tubes were incubated for 15 min at room temperature in the dark. Two milliliter of Versalyse containing 50 µl of fixative solution was then added prior to another incubation of 15 min at room temperature in the dark. Cells were centrifuged 6 min at 250*g*, resuspended in 3 ml of 1× PBS and centrifuged again. The pellet was finally resuspended in 250 µl of 1× PBS and stored at 4°C without light until the acquisition on a cytometer within the next 24 h.

Clinical Absolute Counts Determination for Main Lymphocytes Populations

Lymphocyte blood cells (CD3+, CD4+, CD8+ T lymphocytes, CD19+ B lymphocytes, and CD3-CD56+ NK cell) counts (cells/µl) were established from fresh blood samples using CYTO-STAT tetraCHROME kits with Flowcount fluorescents beads as internal standard and tetra CXP software with a FC500 cytometer according to manufacturer's instructions (Beckman Coulter).

Flow Cytometry Analyses

Flow cytometry data were analyzed with Kaluza 1.3 software (Beckman Coulter). Statistical analyses were performed using Prism 6.0 (GraphPad) software. The Wilcoxon test was used to compare less than 30 matched pairs. $P < 0.05$ was considered as significant.

Acknowledgments

We thank Michelle Barbié, Cornelia Degbé, and Nathalie Fery for their technical help, and Olivier Jaen from Beckman Coulter for his help in the design of cytometry panels.

Literature Cited

1. Miyara M, Gorochov G, Ehrenstein M, Musset L, Sakaguchi S, Amoura Z. Human FoxP3+ regulatory T cells in systemic autoimmune diseases. Autoimmun Rev 2011; 10:744–755.
2. Tanaka A, Sakaguchi S. Regulatory T cells in cancer immunotherapy. Cell Res 2017; 27:109–118.
3. Yang Y. Cancer immunotherapy: Harnessing the immune system to battle cancer. J Clin Invest 2015;125:3335–3337.
4. Weber JS. Biomarkers for checkpoint inhibition. Am Soc Clin Oncol Educ Book 2017;37:205–209.
5. Maecker HT, McCoy JP. A model for harmonizing flow cytometry in clinical trials. Nat Immunol 2010;11:975–978.
6. McGonagle D, McDermott MF. A proposed classification of the immunological diseases. PLoS Med 2006;3:e297.
7. Lorenzon R. Clinical and multi-omics cross-phenotyping of patients with autoimmune and auto-inflammatory diseases: The observational case-controlled TRANSIMMUNOM study. BMJ Open. (in press; http://dx.doi.org/10.1136/bmjopen-2017-021037).
8. Champiat S, Lambotte O, Barreau E, Belkhir R, Berdelou A, Carbonnel F, Cauquil C, Chanson P, Collins M, Durrbach A, et al. Management of immune checkpoint blockade dysimmune toxicities: A collaborative position paper. Ann Oncol 2016;27:559–574.
9. Chaput N, Lepage P, Coutzac C, Soularue E, Le Roux K, Monot C, Boselli L, Routier E, Cassard L, Collins M, et al. Baseline gut microbiota predicts clinical response and colitis in metastatic melanoma patients treated with ipilimumab. Ann Oncol 2017;28:1368–1379.
10. Mahnke Y, Chattopadhyay P, Roederer M. Publication of optimized multicolor immunofluorescence panels. Cytometry Part A 2010;77A:814–818.
11. Maecker HT, McCoy JP, Nussenblatt R. Standardizing immunophenotyping for the Human Immunology Project. Nat Rev Immunol 2012;12:191–200.
12. Maecker HT, Frey T, Nomura LE, Trotter J. Selecting fluorochrome conjugates for maximum sensitivity. Cytometry Part A 2004;62A:169–173.
13. Tripodi D, Lyons S, Davies D. Separation of peripheral leukocytes by Ficoll density gradient centrifugation. Transplantation 1971;11:487–488.
14. Draxler D f, Madondo M t, Hanafi G, Plebanski M, Medcalf R l. A flowcytometric analysis to efficiently quantify multiple innate immune cells and T Cell subsets in human blood. Cytometry Part A 2017;91A:336–350.
15. Appay V, Reynard S, Voelter V, Romero P, Speiser DE, Leyvraz S. Immuno-monitoring of CD8+ T cells in whole blood versus PBMC samples. J Immunol Methods 2006;309:192–199.
16. Brodie T, Brenna E, Sallusto F. OMIP-018: Chemokine receptor expression on human T helper cells. Cytometry Part A 2013;83A:530–532.
17. Renzi P, Ginns LC. Analysis of T cell subsets in normal adults. Comparison of whole blood lysis technique to Ficoll–Hypaque separation by flow cytometry. J Immunol Methods 1987;98:53–56.
18. Rajab A, Axler O, Leung J, Wozniak M, Porwit A. Ten-color 15-antibody flow cytometry panel for immunophenotyping of lymphocyte population. Int J Lab Hematol 2017;39(Suppl 1):76–85.
19. Pitoiset F, Barbié M, Monneret G, Braudeau C, Pochard P, Pellegrin I, Trauet J, Labalette M, Klatzmann D, Rosenzwajg M. A standardized flow cytometry procedure for the monitoring of regulatory T cells in clinical trials. Cytometry B Clin Cytom 2018; DOI: 10.1002/cyto.b.21622.
20. Jamin C, Le Lann L, Alvarez-Errico D, Barbarroja N, Cantaert T, Ducreux J, Dufour AM, Gerl V, Kniesch K, Neves E, et al. Multi-center harmonization of flow cytometers in the context of the European "PRECISESADS" project. Autoimmun Rev 2016;15:1038–1045.
21. Gattinoni L, Speiser DE, Lichterfeld M, Bonini C. T memory stem cells in health and disease. Nat Med 2017;23:18–27.
22. Consuegra-Fernández M, Aranda F, Simões I, Orta M, Sarukhan A, Lozano F. CD5 as a target for immune-based therapies. Crit Rev Immunol 2015;35:85–115.
23. Peretz Y, He Z, Shi Y, Yassine-Diab B, Goulet J-P, Bordi R, Filali-Mouhim A, Loubert J-B, El-Far M, Dupuy FP, et al. CD160 and PD-1 co-expression on HIV-specific CD8 T cells defines a subset with advanced dysfunction. PLoS Pathog 2012;8:e1002840.
24. Brenchley JM, Karandikar NJ, Betts MR, Ambrozak DR, Hill BJ, Crotty LE, Casazza JP, Kuruppu J, Migueles SA, Connors M, et al. Expression of CD57 defines replicative senescence and antigen-induced apoptotic death of CD8+ T cells. Blood 2003;101:2711–2720.
25. Mahnke YD, Beddall MH, Roederer M. OMIP-017: human CD4(+) helper T-cell subsets including follicular helper cells. Cytometry Part A 2013;83A:439–440.
26. Churlaud G, Pitoiset F, Jebbawi F, Lorenzon R, Bellier B, Rosenzwajg M, Klatzmann D. Human and Mouse CD8(+)CD25(+)FOXP3(+) Regulatory T Cells at Steady State and during Interleukin-2 Therapy. Front Immunol 2015; 6:171.

27. Lecendreux M, Churlaud G, Pitoiset F, Regnault A, Tran TA, Liblau R, Klatzmann D, Rosenzwajg M. Narcolepsy type 1 is associated with a systemic increase and activation of regulatory T cells and with a systemic activation of global T cells. PLoS One 2017;12:e0169836.
28. Sims GP, Ettinger R, Shirota Y, Yarboro CH, Illei GG, Lipsky PE. Identification and characterization of circulating human transitional B cells. Blood 2005;105:4390–4398.
29. Kern DJ, James BR, Blackwell S, Gassner C, Klein C, Weiner GJ. GA101 induces NK-cell activation and antibody-dependent cellular cytotoxicity more effectively than rituximab when complement is present. Leuk Lymphoma 2013;54:2500–2505.
30. Chirumbolo S, Bjorklund G, Vella A. Using a CD45dim/CD123bright/HLA-DRneg phenotyping protocol to gate basophils in FC for airway allergy. CD123 does not decrease. Adv Respir Med 2017;85:193–201.
31. Streitz M, Miloud T, Kapinsky M, Reed MR, Magari R, Geissler EK, Hutchinson JA, Vogt K, Schlickeiser S, Kverneland AH, et al. Standardization of whole blood immune phenotype monitoring for clinical trials: panels and methods from the ONE study. Transp Res 2013;2:17.
32. Hasan M, Beitz B, Rouilly V, Libri V, Urrutia A, Duffy D, Cassard L, Di Santo JP, Mottez E, Quintana-Murci L, et al. Milieu Intérieur Consortium. Semi-automated and standardized cytometric procedures for multi-panel and multi-parametric whole blood immunophenotyping. Clin. Immunol 2015;157: 261–276.
33. Shikhagaie MM, Germar K, Bal SM, Ros XR, Spits H. Innate lymphoid cells in auto-immunity: Emerging regulators in rheumatic diseases. Nat Rev Rheumatol 2017;13: 164–173.